Towards a unified solution method for fluid-structure interaction problems : progress and challenges

Proceedings of PVP 2006-ICPVT11
10th International Symposium on Emerging Technology in Fluids, Structures and Fluid-Structure Interactions
July 23-27, 2006, Vancouver, BC, Canada

PVP2006-ICPVT11-93354

TOWARDS A UNIFIED SOLUTION METHOD FOR FLUID-STRUCTURE INTERACTION PROBLEMS: PROGRESS AND CHALLENGES

G. Papadakis
Experimental and Computational Laboratory for the Analysis of Turbulence
Department of Mechanical Engineering
King's College London, Strand WC2R 2LS, UK
Email: george.papadakis@kcl.ac.uk

C. G. Giannopapa
Dept. of Mathematics and Computer Science
Technische Universiteit Eindhoven
PO Box 513, 5600 MB Eindhoven
The Netherlands
Email: c.g.giannopapa@tue.nl

ABSTRACT

The paper presents the progress in the development of a novel unified method for solving coupled fluid-structure interaction problems as well as the associated major challenges. The new approach is based on the fact that there are four fundamental equations in continuum mechanics: the continuity equation and the three momentum equations that describe Newton's second law in three directions. These equations are valid for fluids and solids, the difference being in the constitutive relations that provide the internal stresses in the momentum equations: in solids the stress tensor is a function of the strain tensor while in fluids the viscous stress tensor depends on the rate of strain tensor. The equations are written in such a way that both media have the same unknown variables, namely the three velocity components and pressure. The same discretisation method (finite volume) is used to discretise the four partial differential equations and the same methodology to handle the pressure-velocity coupling. A common set of variables as well as a unified discretisation and solution method leads to a strong coupling between the two media and is very beneficial for the robustness of the algorithm. Significant challenges include the derivation of consistent boundary conditions for the pressure equation in boundaries with prescribed traction as well as the handling of discontinuity of pressure at the fluid-structure interface.

INTRODUCTION

Fluid-structure interaction (FSI) occurs in many areas of engineering (aerospace, civil or mechanical) as well as other scientific disciplines including medicine, biomechanics etc. FSI analysis becomes crucial when the deformation of a fluid boundary, for example a vessel, can not be neglected. During this interaction, the pressure and the viscous stresses of the fluid act on the solid boundary and lead to structural deformations, which in turn affect the fluid flow and consequently the velocities, pressure and viscous stresses of the fluid. Thus the response of the system can only be determined if the coupled problem is solved. In the case of liquids, which are almost incompressible, even a small structural deformation can have a significant effect. For example, the cross sectional area of a typical plastic pipeline may expand by, say, 0.1% during a surge event but it is this expansion that causes the pressure surge to travel three times slower than in a perfectly rigid pipe. In the case of blood flow in arteries, which are extremely flexible, the wave speed is 200 times slower than in an equivalent rigid tube.

In the conventional approach for simulating fluid-structure interaction problems, the fluid and solid components are treated separately and information is exchanged at their interface. The solution of the set of equations for solids provides the three node displacements and the solution of equations for fluids provides the three velocity components and pressure. In this approach, within one time step, the fluid equations are solved and the pressure and viscous stresses become the boundary conditions for the solid equations. These are then solved and from the calculated displacements a new computational domain is obtained in which the fluid equations are solved again. This process is repeated until both sets of equations converge to within a prescribed tolerance. Only then is the procedure advanced to the next time step. This is the fundamental idea of the monolithic methods.

Different discretisation methods are traditionally used for the solution of the two sets of equations. For structures, the finite

element method is very well established, has sound mathematical formulation and has been used very successfully for decades [1,2]. On the other hand, the finite volume discretisation method for the fluids equations is still the most widely used method in the CFD community [3]. The exchange of information between the two different solution methods that solve for different variables with different discretisation methods is not a trivial task. It has also known drawbacks such as high computational cost and potential numerical instability, especially if the structural displacements are not small. An additional drawback is that one has to maintain two solution algorithms and an interface between them.

Against this background, the main objective of the paper is to present the development of a novel, unified formulation for the numerical modelling of coupled fluid-structure interaction problems. In order to derive a unified formulation, two issues have to be addressed carefully: first the two sets of equations for fluids and structures should be cast in the same form and second a common discretisation and solution method must be used. These two issues are dealt with in the following sections. Challenges that were encountered during the development of the method will be also highlighted and discussed.

MATHEMATICAL FORMULATION

It is well known that there are four fundamental equations in continuum mechanics: the continuity equation and the three momentum equations that describe Newton's second law in three directions [4,5]. These equations are shown below:

$$\frac{\partial \rho}{\partial t} + \nabla \cdot (\rho \vec{U}) = 0 \tag{1}$$

$$\frac{\partial \rho \vec{U}}{\partial t} + \nabla \cdot (\rho \vec{U}\vec{U}) = \nabla \cdot \sigma \tag{2}$$

As it can be seen, these four equations are expressed in terms of velocities and are valid for both fluids and solids. The difference lies in the constitutive relation that provides the stresses (σ): in solids the stress tensor is a function of the strain tensor while in fluids the viscous stress tensor depends on the rate of strain tensor. More specifically, for a linear elastic (or Hookean) solid σ is given by:

$$\sigma = 2\mu\varepsilon + \lambda tr(\varepsilon) I \tag{3}$$

where ε is the strain tensor defined by

$$\varepsilon = 1/2(\nabla D + \nabla D^T) \tag{4}$$

and D is the displacement.

Substituting equation (4) into (3), the stress tensor can be written in terms of displacement as:

$$\sigma = \mu \nabla D + \mu (\nabla D)^T + \lambda tr(\nabla D) I \tag{5}$$

For a linear viscous (or Newtonian fluid) σ is given by:

$$\sigma = 2\eta dev(\dot{\varepsilon}) - pI \tag{6}$$

where $\dot{\varepsilon}$ is the strain rate tensor and dev(.) denotes the deviatoric part of a tensor.

Since equations (1) and (2) that describe the fundamental physical laws are written in terms of velocities, it is reasonable to use velocities as unknown variables for both solids and fluids. For fluids, the primitive variable approach (i.e. velocity-pressure formulation) is now almost universally used. So the equations for the solid medium have to be reformulated in such a way as to contain the same variables. The way that this is achieved is explained in the next section.

Velocity-pressure formulation for solids

Velocity and displacement are linked with the following equation:

$$\vec{U} = \frac{d\vec{D}}{dt} \tag{7}$$

and therefore the displacement components can be obtained by integrating equation (7). In the present paper the trapezoidal rule is used (see Figure 1):

$$\vec{D} = \int_{t_0}^{t+\Delta t} \vec{U}\, dt = \vec{D}_\Sigma + \frac{\Delta t}{2}\left[\vec{U}^n + \vec{U}^o\right] \tag{8}$$

where the superscripts (n) and (o) denote the new and old time step respectively.

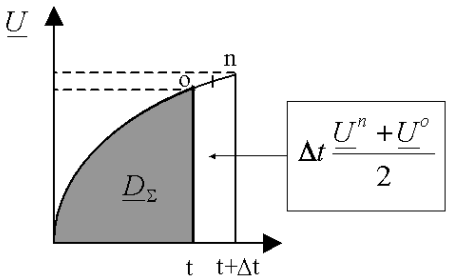

Figure 1: Integration of velocity

Substituting equation (8) into (5) and the result in (2) a velocity-based formulation for the momentum equation is obtained:

$$\frac{\partial \rho \vec{U}}{\partial t} = \frac{\Delta t}{2} \nabla \cdot \left[\mu \nabla \vec{U} + \mu (\nabla \vec{U})^T + \lambda tr(\nabla \vec{U}) I \right] + \nabla \cdot \vec{\Sigma}^+ \quad (9)$$

where the tensor $\vec{\Sigma}^+$ contains the contribution of the 'old' time instant. Note that in order to derive this equation, it was assumed that the convection term in equation (2) is negligible because of small deformations.

The (hydrostatic) pressure p in solids is defined as $p = -\frac{1}{3} tr(\sigma)$ where σ is the stress tensor and tr(.) is the trace operator [1]. It can be seen that equation (9) does not contain pressure. In fact, the solution of (9) can provide the velocities, from which the displacements can be obtained from equation (8) and the pressure can be evaluated from:

$$p = -K \cdot \varepsilon_v = -K \cdot tr(\varepsilon) \quad (10)$$

where K is the bulk modulus ($K = \lambda + \frac{2}{3}\mu$) and ε_v is the dilatation. However, this method of evaluating pressure does not work for incompressible solids simply because the bulk modulus tends to infinity, the dilatation to zero but their product (i.e. pressure) is finite. In finite element formulation, this creates the node-locking problem [1], which is resolved by treating pressure as a separate unknown variable. It is also possible to treat pressure as unknown even for compressible solids [1, 2]. This leads to a formulation that is valid for both compressible and incompressible behavior and is the one adopted in the present work.

The stress tensor σ is split into the hydrostatic and deviatoric part as follows:

$$\sigma = dev(\sigma) - pI \quad (11)$$

This equation in combination with (5) and (8) leads to the following momentum equation that contains velocity and pressure as independent variables:

$$\frac{\partial \rho U}{\partial t} = \frac{\Delta t}{2} \nabla \cdot \left[\mu \nabla U + \mu (\nabla U)^T + \frac{2}{3} \mu tr(\nabla U) I \right] + \nabla \cdot dev\Sigma^+ - \nabla p \quad (12)$$

The additional equation from which pressure is obtained is the continuity equation. This equation contains density and velocity but it can be converted to an equation for pressure by noting that the density and pressure are linked with the barotropic relation:

$$\frac{\partial \rho}{\partial p} = \frac{\rho}{K} \quad (13)$$

where K is the bulk modulus. For small variations in pressure about a reference pressure p_0, equation (13) can be linearised as:

$$\rho \approx \rho_0 \left[1 + (p - p_0)/K \right] \quad (14)$$

For the special case of incompressible solid, the density of the solid is constant and the first term on the left hand side of equation (1) is zero. For this case, the continuity equation contains only velocities. In fact, the pressure must be calculated in such a way as to yield a displacement (and therefore a velocity) field with zero divergence. This is exactly the role of pressure for incompressible fluids as well.

DISCRETISATION METHOD

Having decided on the form of the equations as well as the unknown variables, the second issue is now addressed, i.e. the selection of a common discretisation and solution method.

As mentioned earlier, the finite element method dominates the area of structural mechanics. The method is based on the variational principle, uses predefined shape functions depending on the topology of the element and can be easily extended to higher order discretisation. For the solution of a partial differential equation, the finite element method produces large block matrices and relies on direct system solvers. The finite volume method on the other hand is based on the integral form of partial differential equations, is usually second order accurate in space and time and uses segregated solution procedures i.e. the equations are solved sequentially, one after the other, until convergence of the whole system is achieved.

In the finite volume method, the cross-component coupling terms are treated explicitly. Thus the choice of a direct solver over a segregated solver for a linear elastic problem lies mainly in the trade-off between the high expense of the former approach for large matrices and the cheaper iterative solvers with the necessary iteration over the explicit cross-component coupling for the latter.

The finite volume method is inherently good at treating the complicated, coupled, non-linear partial differential equations that describe the motion of fluid flows. In recent years, calculations using several million cells are regularly reported. In order to keep the computational time within acceptable limits, remarkable improvements in the performance of the method have been made. For example, modern finite volume solvers are fully parallelised and can use massively parallel computers with thousand CPUs. In the present work, the finite volume method was used to discretise all equations.

The momentum equation in a semidiscretised form can be written as:

$$\alpha_P U_P = H(U) - \nabla p \tag{15}$$

where H(U) contains the contributions of the surrounding nodes, previous time step as well as all other source terms except pressure. Substituting equations (15) and (14) into the continuity equation (1) and setting $\psi=\rho_0/K$, a new PDE for pressure can be obtained:

$$\frac{\partial \psi p}{\partial t} + \nabla \cdot \left[(\rho_0 - \psi p_0) \frac{H(U)}{\alpha_P} \right] + \nabla \cdot \left[\psi p \frac{H(U)}{\alpha_P} \right] - \nabla \cdot \left[\frac{\rho}{\alpha_P} \nabla p \right] = 0 \tag{16}$$

In order to ensure that the velocity field satisfies the continuity equation, the PISO algorithm was adopted [6]. The PISO algorithm is most suitable for transient problems and can be used for compressible as well incompressible flows in an iterative manner. This solver has been widely used in fluids, but it can now be used for solids as well since we have the same pressure-velocity formulation. For the evaluation of velocities at the faces of the control volumes, the Rhie and Chow interpolation method is employed [12].

For the discretisation of the spatial terms, second order accurate central approximations are used. For the time marching, the first order accurate Euler method as well as a three-level scheme has been employed. A linear stability analysis of the diffusion and dispersion characteristics of these discretisation schemes when applied to the one dimensional wave equation can be found in [9]. Comparative results between these two time marching schemes are provided in the results section.

Boundary conditions

The implementation of the boundary conditions for fluids is well known. For solids there are two types of boundary conditions: prescribed displacement or traction. Care should be taken in the consistent implementation of these conditions for the reformulated solids equations, especially for the pressure equation as explained below.

The first type (prescribed displacement) results in Dirichlet condition for velocity. As for pressure, there is no need for a boundary condition, as the value of pressure at the boundary does not enter into the discretised continuity equation when the boundary velocity is prescribed.

For the second type (prescribed traction), the boundary condition for the momentum equation is obtained by applying force balance at the boundary. In other words, when the momentum equation is integrated into a control volume and the Gauss divergence theorem is used to convert the volume integral to a surface one, the term that involves the boundary face is equal to the force acting on this face.

For the pressure equation, the boundary condition for prescribed traction is more complicated. In the finite element approach, when the mixed displacement-pressure formulation is used to deal with incompressible solids, both the displacement and the pressure degrees of freedom are unknowns in a large system whose diagonal components corresponding to pressure are zero. The solution of the equations of the complete assemblage of elements needs special considerations to avoid encountering a zero pivot element [1]. Using this approach, no special boundary conditions are needed for pressure. In fact the prescribed displacements and tractions at the boundaries are sufficient to allow the complete determination of displacement and pressure at the interior of the domain.

However, in fluid dynamics the segregated solution approach is usually employed i.e. the equations are solved sequentially one after the other and outer iterations are performed to ensure the convergence of the whole system as already mentioned. Since a unified solution method is sought, the same approach should be used for solids as well and therefore pressure must be obtained from the solution of its own separate equation (16). But this generates the problem of boundary conditions for this equation.

An example will be used to illustrate the difficulty of the problem. Let's consider a circular cylinder subjected to the action of internal gas pressure p_{fi}. The internal radius of the cylinder is r_i and its thickness is h, as shown in figure 2. Assume for simplicity that the gas inside the cylinder is at rest so only the pressure force is acting on the internal cylinder wall. The cylinder has its axial end faces fixed i.e. the problem is plain strain. For this case, the analytic solution for the stress components is [4]:

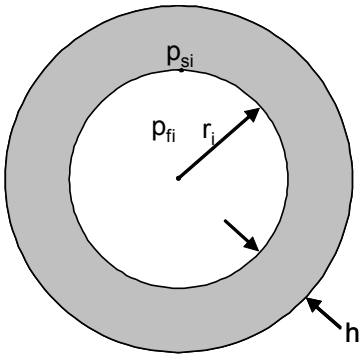

Figure 2: Circular cylinder under internal pressure.

$$\sigma_{rr}(r) = -p_{fi}\frac{\left(\frac{r_i+h}{r}\right)^2 - 1}{\left(\frac{r_i+h}{r_i}\right)^2 - 1}$$
$$\sigma_{\theta\theta}(r) = p_{fi}\frac{\left(\frac{r_i+h}{r}\right)^2 + 1}{\left(\frac{r_i+h}{r_i}\right)^2 - 1} \quad (17)$$
$$\sigma_{r\theta}(r) = 0$$
$$\sigma_{zz}(r) = \nu(\sigma_{rr}(r) + \sigma_{\theta\theta}(r))$$

In order to obtain this analytic solution the following boundary conditions were used at $r=r_i$:

$$\sigma_{rr}(r_i) = -p_{fi}$$
$$\sigma_{rr}(r_i + h) = 0 \quad (18)$$

i.e. the radial stress at the flow-structure interface is determined by the gas pressure. The definition of pressure for solids $p = -\frac{1}{3}(\sigma_{rr} + \sigma_{\theta\theta} + \sigma_{zz})$ can now be used to determine its value at the interface, p_{si} (see figure 2). It can be shown easily that the solid and fluid pressures are not continuous at the interface. In fact, while the radial component of the stress σ_{rr} is compressive and varies from 0 to p_{fi}, the circumferential stress $\sigma_{\theta\theta}$ is tensile and can be many times larger than p_{fi} for thin tubes.

Returning now to the problem of pressure boundary condition, it can be seen that the solid pressure at the interface is unknown. By definition, it depends on the normal as well as the tangential stresses at the boundary and the specification of an appropriate boundary condition is a major challenge.

It must be noted at this point that this is the first time a pressure equation is employed for solids and therefore there is no information available in the open literature. However, the problem of consistent boundary conditions for pressure has received considerable attention in fluid mechanics. In [7] a carefully derived boundary condition for pressure is obtained. A similar approach is followed in the present work i.e. the (vector) momentum equation is projected to the unit vector normal to the traction boundary and an expression for the pressure normal gradient is obtained that is used as boundary condition for the pressure equation. The analytic equations are provided in [10]. Through the cross-component coupling, the momentum equations contain implicit information on the stress distribution in the boundary normal as well as the tangential directions and this information is retained in the expression of the pressure boundary condition. To the best of the authors' knowledge, this is the first time that this type of boundary condition is used in solid mechanics.

DESCRIPTION OF TEST CASE

The aforementioned methodology and boundary conditions are validated against a transient beam-bending problem. This case comprises both normal as well shear stresses. Figure 3 shows a schematic representation of the case considered.

The cantilevered beam is deflected from the horizontal position by applying at the right end a shear stress $\tau = 10^6\,Pa$ and is then released. The upper and lower surfaces of the beam are free traction boundaries. The beam specifications are shown in Table 1.

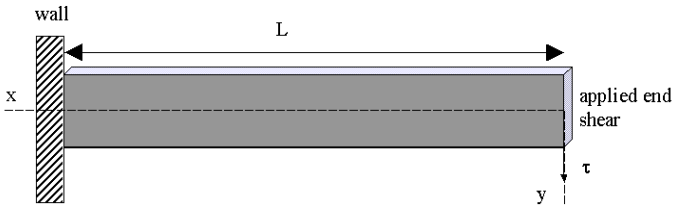

Figure 3: Two dimensional beam.

Property	Value
Modulus (E)	$4x10^9$ Pa
Poisson ratio (ν)	0.3
Density (ρ)	1450 Kg/m^3
Length (L)	20m
Height (h)	5m
Depth (w)	1m

Table 1: Material properties and dimensions of the beam.

A two-dimentional analytical solution for the steady state of the maximum end displacement at x=0 is given by [8]:

$$\delta = \frac{4\tau}{E}\frac{L^3}{h^2}\left[1 + \frac{3}{4}(1+\nu)\left(\frac{h}{L}\right)^2\right] \quad (19)$$

In order to calculate the main frequency of oscillation of the beam, a one-dimensional approximation is used for which an analytical solution is available. Thus, the 1D solution is used only as a rough reference guide to validate the computational results. The fundamental eigenfrequency of the undamped oscillation is:

$$\omega^2 = 1.875^4\frac{Eh^2}{12\rho L^4} \quad (20)$$

For the present case, the end displacement is δ = 0.340 m, the oscillation frequency is $f = \omega/2\pi = 3.35$ Hz and the propagation of the stress wave through the beam is $c = \sqrt{E/\rho} = 1660 m/\sec$.

RESULTS AND DISCUSSION

The time integration scheme used for equation (12) was first-order Euler implicit. A 40x10 mesh was used with a time step $\Delta t = 10^{-4}$s corresponding to Courant number Co=0.33. Convergence was achieved using two PISO loops and four external pressure-velocity loops for each time step. The solution gives a sinusoidal oscillation of the beam about the mean static deflection.

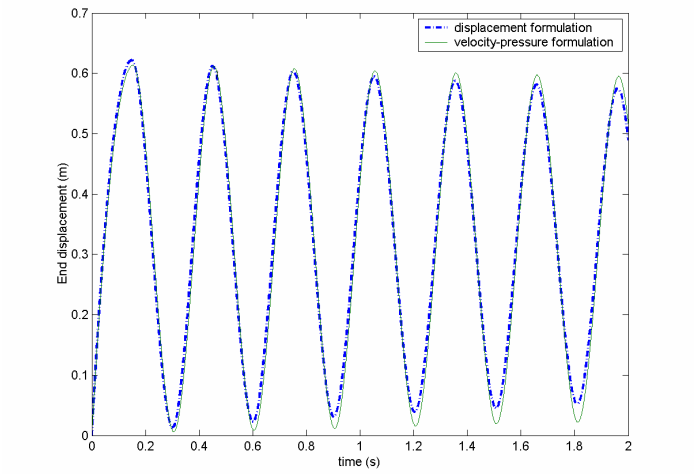

Figure 4: Comparison of end displacement obtained with the standard stress analysis and the velocity-pressure formulation (Co=0.33).

The beam oscillates with a frequency of 3.32Hz and with maximum and mean deflections of 0.62m and 0.31m, respectively. The calculated values are quite close to the values from the analytical solution, which predicts a maximum deflection of 0.68m and an oscillation frequency of 3.35Hz, as already mentioned.

A comparison between the standard displacement formulation and the new velocity-pressure formulation is shown in Figure 4. For the standard stress analysis formulation, the finite volume method was used with a second-order central discretisation scheme in space and a first-order accurate scheme in time. The results obtained using the two formulations agree quite well. This shows that the velocity-pressure approach with the aforementioned boundary conditions for pressure is a valid one.

The effect of the discretisation scheme used for the first order time derivative of velocity in equation 12 was also investigated. The discretisation schemes compared are the first order Euler Implicit and a three time level method (or Backward Differencing). The latter is a second order accurate scheme and is also frequently used in computational fluid dynamics. In Figure 5 it can be seen that the Backward Differencing scheme is less dissipative that the Euler implicit, as expected. Over a period of 30s (300,000 time steps) the Euler Implicit dissipated about 14.7% and over 100 s (1,000,000 time steps) about 33.3%. On the other hand the Backward Differencing over a 30 s period has much smaller dissipation.

The accuracy can be improved further with the decrease of the time step size. Figure 6 compares different time step sizes for Euler Implicit discretisation scheme. It can be seen that when the time step is decreased from 10^{-4}s to 10^{-5}s (C_0=0.033) the accuracy over a 30s period improves about 7.5 %. When the time step is decreases from 10^{-5}s to 10^{-6}s (C_0=0.0033) there is no significant change, only 0.62% improvement, but the computational overhead is quite substantial.

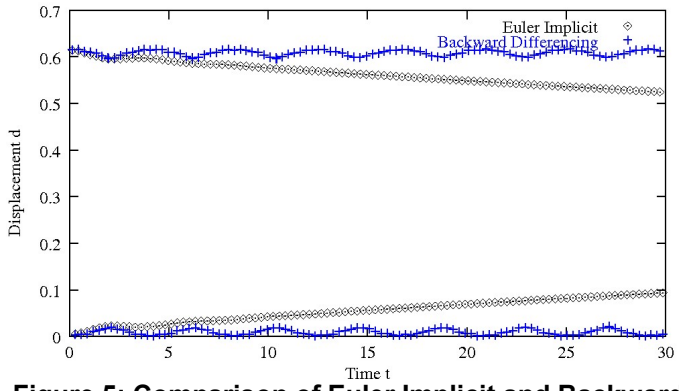

Figure 5: Comparison of Euler Implicit and Backward Differencing scheme (envelope of end displacement).

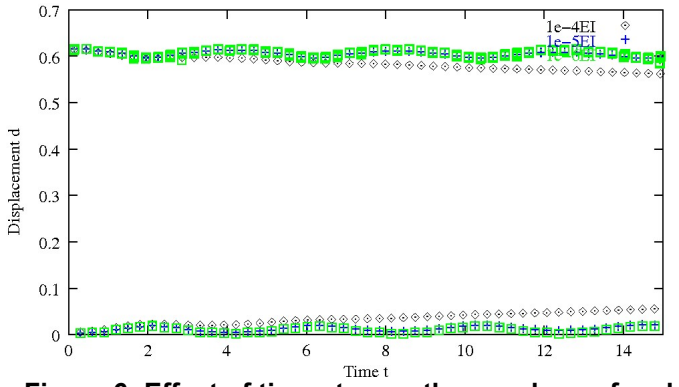

Figure 6: Effect of time step on the envelope of end displacement (Euler Implicit scheme with time steps 10^{-4}s, 10^{-5}s and 10^{-6}s).

The results of the first order accurate Euler Implicit scheme with a decreased time step can be compared with those of the second order accurate Backward Differencing scheme. Figure 7 illustrates that for a period of 30s the results of Backward Differencing with time step 10^{-4}s and Euler Implicit with time step 10^{-5}s are almost identical. The Backward differencing

scheme with 10^{-4}s time step is 1.2% less dissipative than the Euler Implicit with 10^{-5}s time step.

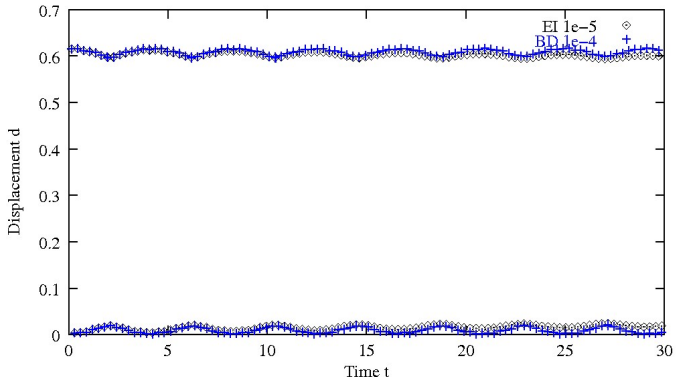

Figure 7: Comparison of envelop of end displacement obtained with Euler Implicit (time step 10^{-5}s) and Backward differencing (time step 10^{-4}s).

A parametric study was also undertaken with different beam dimensions. The conditions, the predicted and analytic results as well as their differences are shown in table 2.

In all cases the time step used was Δt=10^{-4}s, the temporal discretisation scheme applied was Backward differencing and the mesh resolution Δx was kept constant. For example, for the case with 10m beam length the mesh used was 20x10cells. The end displacement is shown in figure 8. The percentage differences between the analytic solution and the predictions for this case are slightly above 10% as shown in Table 2. It must be noted however that as the analytical solution is 1D, the shorter the beam is in relation to its height, the less accurate the solution would be.

Variable	Analytical	Predicted	% Difference
Beam dimensions: 10mx5m; end shear: 10^6 Pa			
Max Dispacement [m]	0.0995	0.0866	12.96
Frequency [Hz]	13.41	11.64	13.29
Beam size: 20mx5m; end shear: 10^6 Pa			
Max Dispacement [m]	0.68	0.62	8.82
Frequency [Hz]	3.35	3.32	0.9
Beam size: 40mx5m; end shear: 10^6 Pa			
Max Dispacement [m]	5.2	4.72	9.21
Frequency [Hz]	0.84	0.86	2.05

Table 2: Comparison between analytical and computational solutions for beams with different dimensions.

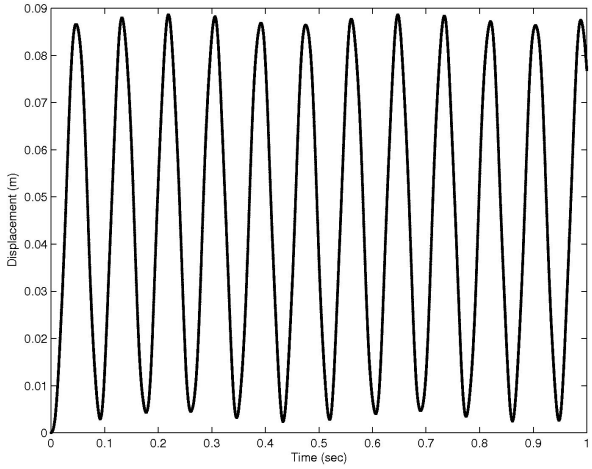

Figure 8: End displacement for a beam with dimensions 10mx5m.

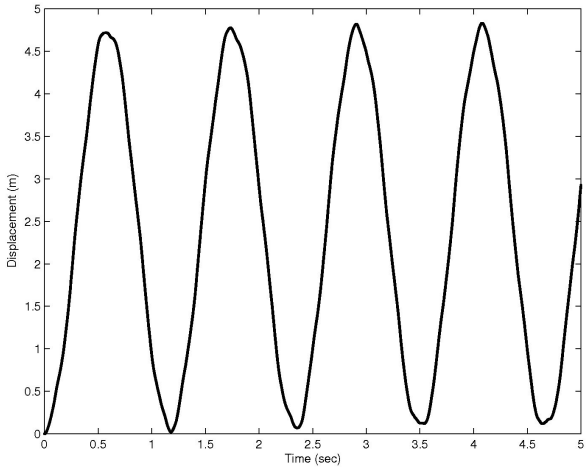

Figure 9: End displacement for a beam with dimensions 40mx5m.

For the case with double the beam length (40mx5m) the mesh used was 80x10cells (Figure 9). The end displacement was 4.72m and the frequency was 0.86 Hz. The percentage difference between the analytical and the numerical solution is 2.05 % for the frequency and 9.21% for the displacement (Table 2). More results can be found in references [9, 10,11].

CONCLUSIONS

A unified solution method was presented suitable for fluid-structure interaction problems with no approximations made to the basic continuum model for Hookean solids and Newtonian fluids. The principal idea is that the fluid and structural behavior is described by a set of equations that has as primitive variables velocity and pressure. The pressure-velocity coupling is handled using the PISO algorithm. Since pressure is used as an independent variable, the study of structural deformations of

fully incompressible solids is straightforward while well-known problems such as node locking are avoided.

It was shown that the pressure at the fluid-structure interface is discontinuous and this poses challenges for the consistent boundary condition for the pressure equation. An approach similar to one used in fluid mechanics was employed.

The solution method for FSI was validated against a transient beam bending test case. The solution method was stable and results close to the analytic solution or to the standard displacement formulation were obtained. It was shown that the unified solution method is capable of solving standard solid mechanics problems with sufficient accuracy. The next step of this work is the application of this method to full FSI problems.

ACKNOWLEDGMENTS

The authors would like to thank EPSRC (research grant GR/N65769) for funding this project and Nabla Ltd.

NOMENCLATURE

Roman symbols

Co	-	Courant number
D	m	displacement
f	Hz	frequency
h	m	beam height/ cylinder thickness
I	-	unit tensor
K	Pa	bulk modulus
L	m	beam length
p	Pa	pressure
r_i	m	internal cylinder radius
t	s	time
U	m/s	velocity
W	m	beam depth

Greek symbols

Δt	s	time step
Δx	m	grid spacing
δ	m	maximum end displacement
ε	-	strain tensor
ε_v	-	dilatation
E	Pa	Young's modulus
η	m^2/s	dynamic viscosity
λ	Pa	Lame's coefficient
μ	Pa	Lame's coefficient
ν	-	Poison ratio
ρ	kg/m^3	density
σ	Pa	Stress tensor
σ_{ij}	Pa	Elements of the stress tensor
τ	Pa	applied end shear
ω	Hz	frequency of undamped oscillations

REFERENCES

[1] Bathe, K. J., 1997, *Finite element procedures.* Prentice Hall, Englewood Cliffs, New Jersey.

[2] Hughes, T.J.R., 2000, *The finite element method: linear static and dynamic finite element analysis*, Dover Publications, inc.

[3] Ferziger, J.H and Peric, M., 1997, *Computational Methods for Fluid Dynamics*, Springer-Verlag

[4] Lai, W.M., Rubin, D. and Krempl, E., 1993, *Introduction to continuum mechanics*, Butterworth-Heinemann, Third Edition.

[5] Malvern, L.E., 1969, *Introduction to the mechanics of a continuous medium*, Prentice Hall, Englewood Cliffs, New Jersey.

[6] Issa, R. I., 1986, "Solution of the implicit discretised fluid flow equation by operator-splitting", Journal of Computational Physics, **62**, pp 40-65.

[7] Gresho, P.M. and Sani, R.L., 1987, "On pressure boundary conditions for the incompressible Navier-Stokes equations", *International Journal for Numerical Methods in Fluids*, **7**, pp 1111-1145.

[8] Geradin, M., and Rixen, D., 1997, *Mechanical vibrations,* Wiley, Chichester, UK

[9] Giannopapa, C.G. and Papadakis, G., 2006, "Linear stability analysis and validation of a unified solution method for fluid-structure-interaction on a structural dynamic problem" submitted to ASME Journal of Pressure Vessel Technology.

[10] Giannopapa, C. G., 2004, *Fluid-Structure interaction in flexible vessels*, PhD thesis, Department of Mechanical Engineering, King's College London, UK.

[11] Giannopapa, C. G. and Papadakis, G., 2004, "A new formulation for solids suitable for a unified solution method for fluid-structure interaction problems," ASME PVP 2004, San Diego California, July 2004, PVP-Vol. **491-1**, pp. 111-117.

[12] Rhie, C. M. and Chow, W. L., 1983, "A numerical study of turbulent flow past an isolated airfoil with trailing edge separation" *AIAA Journal,* **21**, pp. 1525-1532.